ALTERNATING STRESS-STRAIN FIELDS NEAR A CRACK TIP UNDER CYCLIC LOADING

V. Kharin and J. Toribio

Universidad de La Coruña (ULC)
Departamento de Ciencia de Materiales
ETSI Caminos, Campus de Elviña, 15192 La Coruña, Spain

Abstract. Finite deformation analysis of the cracked elastoplastic panel with a plane-strain crack subjected to mode I (opening) cyclic loading under small scale yielding was performed to elucidate the influence of the load range, load ratio and overload peak on the crack-tip shape and near-tip stress and strain fields. At zero-to-tension constant amplitude loading no evidence of geometric crack closure (contact of the crack faces) at load removals was detected, neither after a single overload peak. Compressive crack-closure stresses at load removals were nearly equal to tensile ones at load maxima, and the extrema of both were located beyond the tip. Cyclically stable evolution patterns of stress, plastic strain and strain energy density established near the crack tip after a couple of loading cycles, their accumulation rates being dependent on load range, load ratio and overload peak.

Resumen. Se presenta un análisis elastoplástico por elementos finitos de una placa en deformación plana con una fisura en modo I sometida a carga cíclica en condiciones de plasticidad a pequeña escala, con el fin de elucidar la influencia del intervalo de carga, factor R y sobrecargas sobre la forma del extremo de la fisura y el estado tenso-deformacional próximo. Con amplitud de carga constante no se aprecia cierre geométrico de fisura (contacto entre sus caras) al descargar, ni después de una sobrecarga. Las tensiones compresivas de cierre de fisura tras la descarga son casi idénticas a las alcanzadas en carga máxima, y los extremos de ambas se hallan a cierta distancia del fondo. Tras dos ciclos de carga se estabilizan las leyes de evolución cíclica de tensión, deformación plástica y densidad de energía de deformación cerca del fondo de la fisura, dependiendo sus tasas de acumulación de la amplitud de carga, factor R y nivel de sobrecargas.

1. INTRODUCTION

Fatigue of materials under alternating loads is the cause of many engineering failures, so that its understanding and characterisation in terms of generally applicable and controllable quantities is considered as a prerequisite for safe engineering design and component maintenance. Fatigue crack growth rate da/dN as material's response, together with appropriate external variables governing crack propagation in a material in every particular geometry-and-loading situation have been appreciated as the key issues in damage tolerant design [1]. Fracture mechanics concepts can be used to establish the factors controlling fatigue crack growth. In particular, when inelastic material behaviour (plasticity, damaging, etc.) is localised in a small near tip domain —the small scale yielding (SSY) case— the concept of linear elastic fracture mechanics and the stress intensity factor K can be expected to work well. The basic relationship may be represented in several equivalent forms such as:

$$\frac{da}{dN} = \mathcal{F}(K_{max},K_{min}) = \widetilde{\mathcal{F}}(\Delta K,R) \qquad (1)$$

where the right hand parts are considered to be material-dependent functions, K_{max} and K_{min} are, respectively, the maximum and minimum K-values of the loading cycle; $\Delta K = K_{max}-K_{min}$ the stress intensity range and $R = K_{min}/K_{max}$ the load ratio. Ample experimental evidence favours the K-approach to fatigue cracking, and several expressions of the fatigue "law" (1) have been proposed, but none is fully capable of describing a variety of peculiarities of fatigue crack growth [1,2].

Micromechanisms of fatigue degradation and rupture are thought to be related to cyclic evolutions of stress and strain [1], whereas the K-pattern can be the controlling parameter but not a direct driver. Then analyses of fine peculiarities of local crack tip stresses and strains are essential for linking easily controllable macroscopic variables such as K with fracture mechanisms, and for development of unified framework for characterisation and prediction of fatigue crack growth.

Numerous models have been developed to reveal the evolution of the near tip situation under cyclic loading. Some of them offered closed-form solutions, although restricted by crucial simplistic assumptions (cf. [3] and reviews in [1,2]). More realistic numerical simulations have been also performed for fatigue cracks, mostly under plane stress conditions (cf. papers [4-9] and references therein). However, the majority of these

studies have been confining to the plastic crack closure hypothesis focusing mainly on the crack opening-closing levels of applied K (external load) and not providing in-depth data on evolutions of stresses and strains. Mentioned simulations of the situation near the tip of a fatigue crack neither accounted for large strains nor paid much attention to the role of plane strain constraint. To the authors' best knowledge, only paper [10] offered limited data on large-strain elastoplastic crack tip situation for a single cycle loading-unloading-reloading. Meanwhile, these matters deserve more attention because all the events relevant to the near tip rupture and crack advance take place in the intensively strained very-near tip zone and are driven by stress-strain state therein, and the situation along the crack front in the interior (even of rather thin components) is closer to plain strain state while near the surface plane stress conditions predominate.

2. BASIC MODELLING ISSUES

The model material is supposed to be rate-independent ideal elastoplastic with von Mises yield criterion. Its characteristics are chosen relevant to typical steels: Young modulus E = 200 GPa, Poisson ratio μ = 0.3, tensile yield stress σ_Y =600 MPa (Using obvious normalisation technique, the solutions are applicable to some similitude class of situations fixed by the ratio σ_Y/E and by the crack tip geometry, cf [11]). The crack has initially parallel flanks and smooth round-shape tip of a width (twice the tip radius) b_0, which seems to be a reasonable approximation (discussion of this matter can be found elsewhere [11], and experimental support in [12]). For medium-strength steels the value b_0 = 5 μm is used [12]. The upper bound for applied K-values is limited to 60 MPam$^{1/2}$ which is appropriate for steels as the range at which fatigue cracking goes on. With these parameters the crack length is taken a = 75 mm to enforce the conditions of K-dominated SSY near the tip. The double-edge-cracked panel (Fig. 1) under uniform stress σ_{app} is considered to make use of the K-solution from the compendium [13] as follows:

$$K = 1.158\ \sigma_{app}\sqrt{\pi\ a} \qquad (2)$$

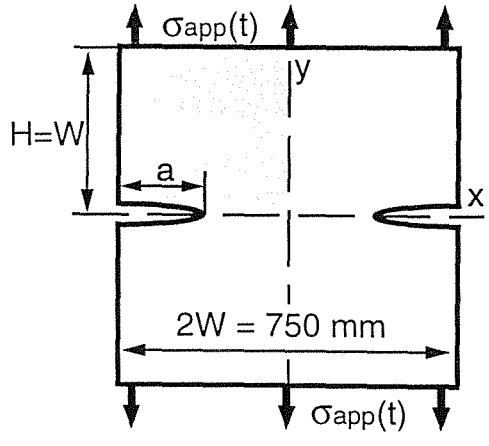

Fig. 1. Schematics of the simulated specimen geometry and loading.

Investigations were performed for several constant amplitude loading patterns at different amplitudes and load ratios. In addition, the effect of a single overload peak was considered. K was a control variable in this study, depending on which corresponding applied load levels σ_{app} were established according to relation (2). The following load cases were used in the numerical simulations:

(I) K_{max} = 60 MPam$^{1/2}$, K_{min} = 0 (i.e., R = 0);

(II) K_{max} = 30 MPam$^{1/2}$, K_{min} = 0 (R = 0);

(III) K_{max} = 60 MPam$^{1/2}$, K_{min} = 30 (R = 0.5);

(IV) K_{max} = 30 MPam$^{1/2}$, K_{min} = 0 (R = 0) with a single overload peak to K_{ov} = 60 MPam$^{1/2}$.

and up to ten loading cycles (twenty load reversals) were completed in each case.

Due to symmetry, the computations were carried out for the one quarter of the panel (shadowed in Fig 1). To avoid excessive distortion of the finite element mesh, and to enable to terminate calculations for several load reversals, the near tip mesh required more refinement than in simulations at rising-only load [11,14]. The load stepping procedure in incremental elastoplastic solution had to be finer than in reported small-strain cycling [6] and large-strain single cycle modelling [10]. Several near-tip mesh refinements were tried, and the optimum one of 1148 four-node quadrilaterals with 1222 nodes was used. The solution of the boundary value problem was accomplished using the nonlinear finite element code MARC [15] with an updated Lagrangian formulation.

3. RESULTS

The shape and size of the near tip plastic zones were found to be in agreement with published data [1-3,5,10]. For all loading cases forward and reverse plastic zones were fairly similar if scaled in corresponding units of $(K_{max,min}/\sigma_Y)^2$, and they remained rather stable with increasing N. The case IV was a little bit specific in that after overload the reverse plastic zone co-related not with the constant amplitude cycle range ΔK but with the overload peak range ΔK_{ov} = K_{ov} − K_{min} and thus it was larger than the forward one after overload.

Near tip crack profiles evolve with load cycling in a similar manner for all load cases. As an example, crack tip deformation corresponding to the load pattern I is depicted in Fig. 2. It should be noted that geometrical crack closure (contact of its faces) was never detected in performed simulations. Crack width at unloading to K = 0 always remained quite considerable, and it never and nowhere returned to the original width b_0. This agrees with another finite-deformation study for a single load removal [10] but contradicts, however, the results of small-strain simulations performed in geometries with growing fatigue cracks [4,6].

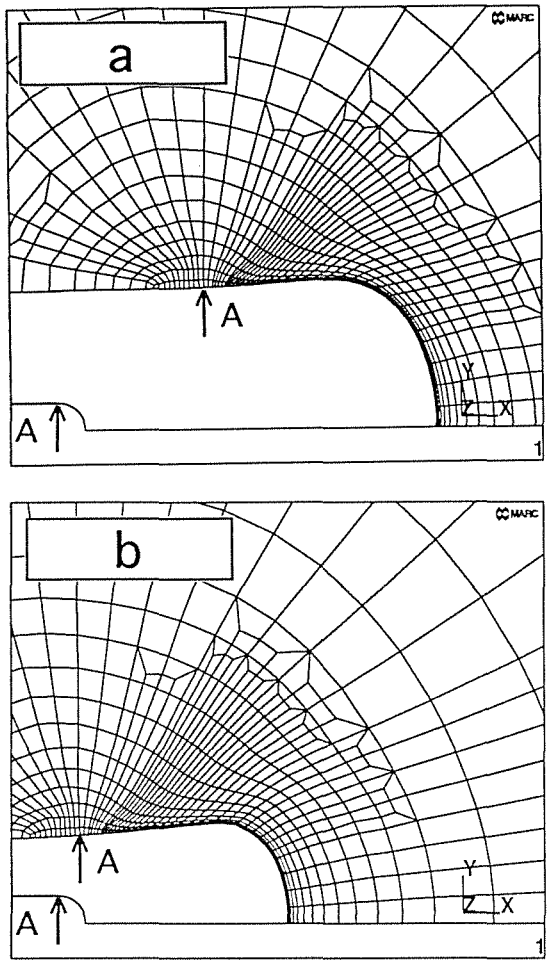

Fig. 2. Near-tip deformations at different stages of load case I: (a) at the 4th maximum load point, $K = K_{max}$; (b) at subsequent unloading point, $K = 0$ (the original crack tip is shown in the bottom left corners).

The values of the crack tip opening displacement (CTOD) δ_t vs. applied K plotted in Fig. 3 are scaled by $\delta_{max} = \delta_t\,(K_{max})$ and K_{max}, respectively, excepting the load case IV for which the overload peak CTOD $\delta_{ov} = \delta_t\,(K_{ov})$ and K_{ov} are in use. The value of δ_t was identified as twice the current vertical displacement of the node A shown in Fig. 2, and the current crack tip width (twice its "radius") is $b = b_0 + \delta_t$. The variability of the crack width along its newly created flanks in the end region (see Fig. 2) is small compared with the width itself, and so, this definition seems to be reasonable. Calculated (K_{max}–δ_t) loops in Fig. 3 demonstrate that the situation in all cases approaches the steady-state cyclic regime.

The near tip stress fields are exemplified in Fig. 4 by the band contours of the normal stress σ_{yy} for the load case I. For other load patterns II – IV, no striking distinctions were observed in the shape and size of the band contours if scaled with respect to the current deformed tip width b, nor spectacular evolutions of them occurred with increasing cycles number N.

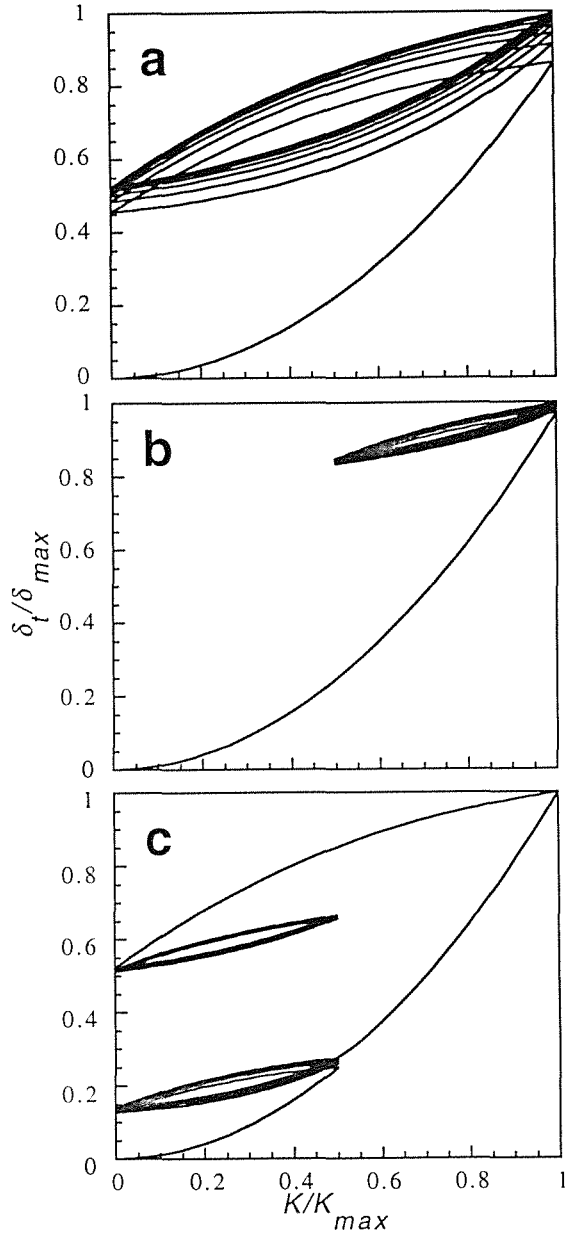

Fig. 3. Variation of CTOD vs. applied K: (a) load case I; (b) load case III; (c) load case IV.

Details on the stress state are given in Fig. 5 where the odd times $t = 2k - 1$ correspond to load maxima and the even ones $t = 2k$ to minima in the k-th cycle, overload (case IV) occurs there at $t = 11$. Stress distributions beyond the tip at similar load cases I and II (the same $R = 0$) are nearly identical if displayed in terms of the distance X of the material point from the tip apex in the original configuration normalised by b. The data apparently confirm preserving under cyclic loading of the notable feature of the crack fields revealed in monotonous loading studies [2,10,11,14], i.e., arising of self-similar (in normalised coordinates) autonomous state governed at similar-shape load patterns just by deformed geometry of the tip and material constants (E and σ_Y in this case). Stress distributions are moderately

sensitive to the load ratio and load sequence. The main distinction between cycling at R = 0.5 (Fig. 5b) from that at R = 0 (Fig. 5a) is accelerated relaxation of the tensile stress beyond the extremum position so that a slight secondary extremum hump can arise. After an overload peak (Fig. 5c) a diminishing of the stress amplitude $\Delta\sigma_{yy} = \sigma_{yy}^{max} - \sigma_{yy}^{min}$ and a sharper drop of σ_{yy} beyond the extremum position are observed.

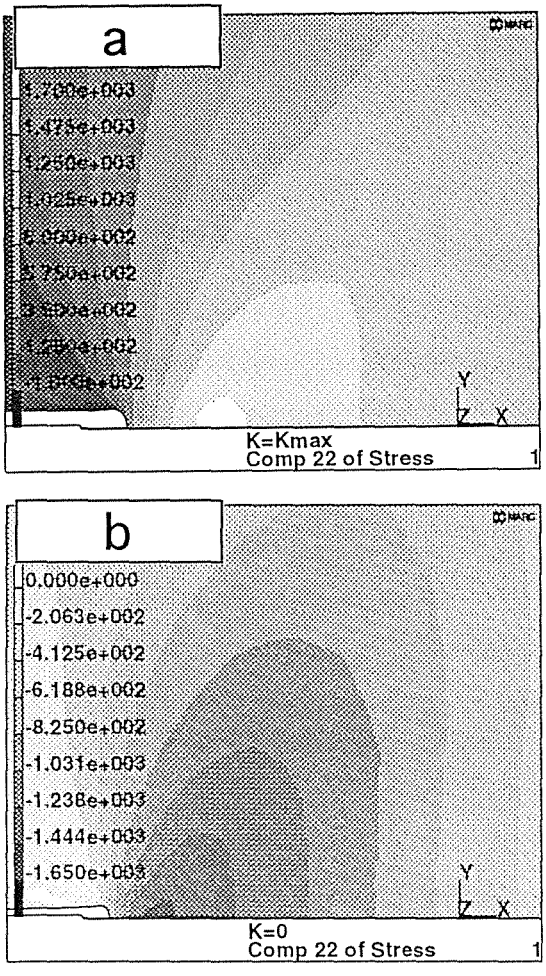

Fig. 4. Distribution of the stress σ_{yy} at load case I: (a) at $K = K_{max}$; (b) at unloading to $K = 0$.

Spatial distributions in the crack tip vicinity of plastic strain components and strain energy density W had no striking peculiarities in load cases I to IV. All of them were similar showing extreme strain concentration in a domain of the size of the order of CTOD, like in rising load large-strain analyses [11,14].

Stress evolutions in material points beyond the tip identified by their coordinates in the original configuration $X_1 = 279b_0 > X_2 = 18b_0 > X_3 = 1.7b_0$ under a sine-shape applied load history are given in Fig. 6. The stress histories far from the tip in the elastic domain and in the periphery of the plastic zone (point X_1) replicate fairly the sine-like alteration of the applied load. The stress history becomes different closer to the tip. After just about the first cycle the $\sigma_{yy}(t)$ acquires a stable cyclic regime as a repetition of nearly the same Π-like shape. This is common for all the load cases. The local load ratio $R_\sigma = \sigma_{yy}^{min}/\sigma_{yy}^{max}$ takes fairly the same value for all them in the immediate vicinity of the tip apex, $R_\sigma(X_3) \approx -1$, irrespective of the remote (applied) R value. The notable peculiarity of the load case IV is that $\Delta\sigma_{yy}$ diminishes locally about 1.5 times after an overload peak. This can be the cause of the known experimental effect of fatigue crack growth retardation after overload, cf. [1,2].

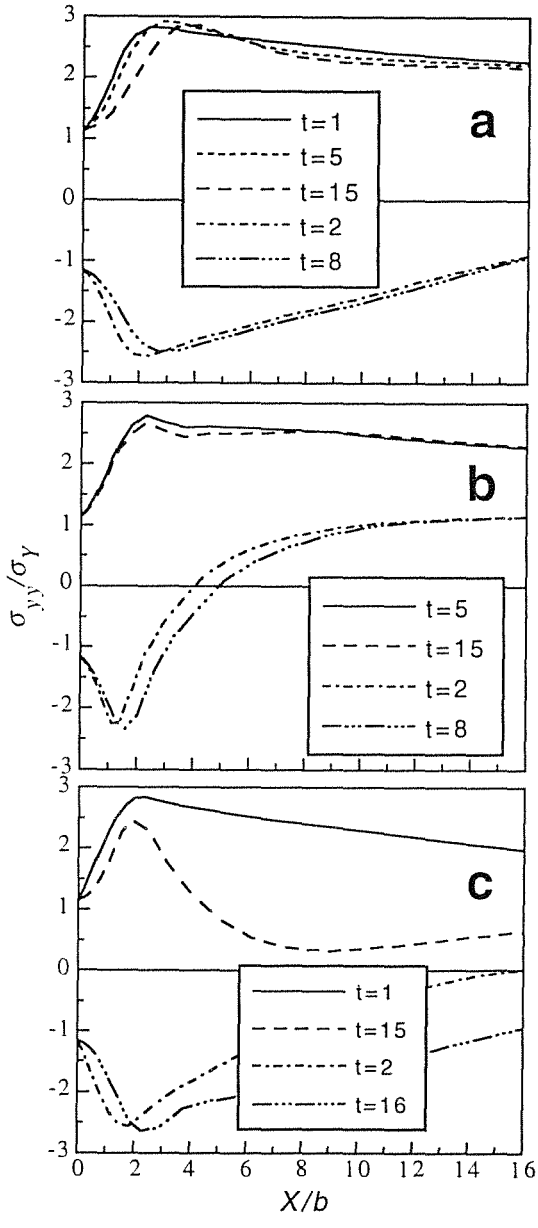

Fig. 5. Normal stress σ_{yy} near the crack tip : (a) at load case I; (b) at load case III; (c) at load case IV.

A certain affinity was found between cyclic evolutions of the near tip plastic tensile strain ε_{yy}^p, equivalent plastic strain ε_{eq}^p, and strain energy density W. They revealed rather similar behaviours. Limiting here only to ε_{yy}^p, we will mark essentially the main features of all. Fig. 7 displays the strain accumulation near the crack tip. These plots display a ratcheting elevation

with alteration "amplitudes" for all load cases in apparent correspondence with their respective ΔK-values. The averaged slopes $\Delta\varepsilon_{yy}{}^{p}/\Delta N$ (secant line from the origin) decrease from one load case to another in the sequence I → III → II → IV (post-overload).

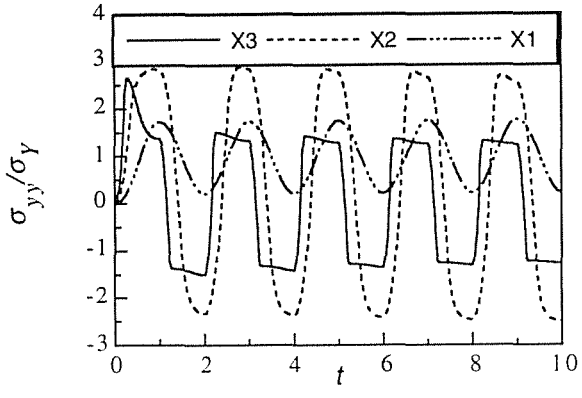

Fig. 6. Evolution of the normal stress σ_{yy} in the points $X_{1,2,3}$ beyond the crack tip at sine-shape applied load alteration (load case I).

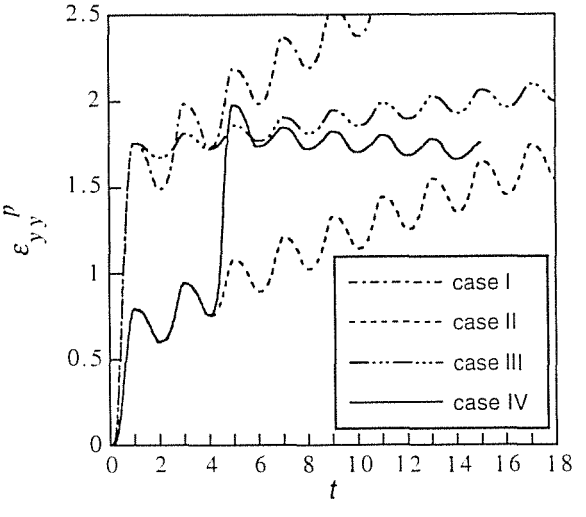

Fig. 7. Plastic strain evolutions in the crack tip (overload peak in the load case IV occurs at t= 5).

4. DISCUSSION

To derive implications for fatigue crack growth from simulations of stress-strain evolution near the crack tip, and to constitute on this basis a tool for crack growth characterisation and prediction, a crack advance criterion is required. For the moment, the majority of simulations of fatigue cracks dealt with arbitrary crack extension schemes with no relevance to the fracture (micro)mechanisms that could really govern crack growth [4-7,9]. Some of them considered possible candidate measures of damage accumulation among stress-, strain- or energy-related variables drawing conclusions in favour of some of them [8]. From the performed simulations it follows that accounting for the mutual affinity, the averaged ratcheting (or "climbing") accumulation behaviours of the three candidates such as $\varepsilon_{yy}{}^{p}$, $\varepsilon_{eq}{}^{p}$ and W, they may have equal opportunities to succeed in monitoring damage accumulation near the crack tip. Although interrelation between the rates of elevation of these "measures" depends on the distance of a material point of interest from the tip, agreement between them can be noticed (cf. Fig. 7) and the observed experimentally trends of variation of the rate of crack growth da/dN depending on peculiarities of applied loading (such as ΔK, R and overload peak) all of them decelerate from one load case to another following the same order I → III → II → IV (post-overload rate).

Concerning the idea about crack closure as an effect responsible for the mentioned trends of crack growth behaviour, modelling of the plane strain crack reported here provides no support for this concept since no signs of closure were detected.

On the other hand, the findings from presented stress-strain analysis with account for geometrical non-linearity, and especially the correlation between plastic strain or energy density accumulation rates and the rates of crack growth mentioned just above yield the following idea: near-tip damage accumulation in fatigue proceeds in some ratcheting manner governed by alternating stress, or strain, or both of them. Then, to establish a firm and general crack growth equation of the kind (1), a promising way seems to be joining of high-resolution stress-strain analysis with the concepts analogous to those used in micromechanical modelling of local fracture near the crack tip to estimate the critical K-value under monotonous loading (see, e.g., [16,17]) on the basis of either critical strain ε_c, or critical absorbed energy density W_c, or adaptation of the critical stress criterion in the manner of local approach of the stress-life type [1], e.g., $\Delta\sigma_{yy} = \sigma_c(N)$, which may be workable because of stabilisation of the near tip stress alteration. Owing to the previously described parallelism between variation of experimental crack growth rate and calculated effective rates of evolution of plastic strains and strain energy density near the crack tip under various loading conditions, this way of developing redictive tools for fatigue crack growth seems to be promising.

5. CONCLUSIONS

High-resolution finite-element analysis of a stationary plane-strain tensile crack in ideal elastoplastic solid under cyclic loading was performed with account for large crack tip geometry changes. Several load cases (histories) were considered to elucidate the effects of the applied load range, load ratio and a single overload peak on the situation near the crack tip. From obtained solutions, the evolutions of the deformed crack tip shape together with the near tip stress and strain characteristics were revealed. At short distance from the tip, i.e., less than approximately $3\delta_{max}$, the stress and strain patterns display important features not captured

neither by small-strain numerical analyses [4-9] nor by simple analytical models [1-3], but similar to finite deformation studies of cracks under rising load. It is important to emphasize that geometrical closure of the crack was never detected. Evolutions of CTOD, remaining always positive, $\delta_t > 0$, approaches steady-state cycling regimes.

Stress and strain distributions in a close vicinity of the crack tip, like in monotonous-load large-strain analyses [11,14], reveal important features for interpretation of the near tip fracture processes. The most notable peculiarities of the near-tip stress fields common for all simulated load cases are the following: (*a*) self-similitude of the spatial distribution of stresses if scaled with respect to the current crack tip width value $b = b_0 + \delta_t$, or $b \approx \delta_t$ at elevated loads, i.e. at greater CTODs; (*b*) establishing of practically steady state regime of cyclic variation after a couple of the first loading cycles, and these stress alterations in the close vicinity of the tip take a specific Π-like tension-compression shapes different from the shape of external load cycling; (*c*) normal stresses near the crack tip attain their extrema —tensile and compressive of nearly equal magnitudes at maximum and minimum external load levels, respectively— noticeably beyond the tip apex.

No-one of the near tip patterns of plastic strain ε_{yy}^p, total equivalent plastic strain ε_{eq}^p or strain energy density W (this latter turns out to be strain-dominated) exhibit saturation, but rather persistent ratcheting or climbing behaviours which may be characterised by certain values of average rates of accumulation dependent on external load range, load ratio and overload peak. The most notable is that these accumulation rates agree with experimentally observable trends of the influence of the external loading characteristics on fatigue crack growth rates.

Performed simulations of the near tip state reveal that the very near tip stress-strain field characteristics, affected by large crack tip deformations (blunting), are apparently able to serve as the measures of damage accumulation near the tip of fatigue crack and are promising as the relevant basis to develop rational procedures for crack behaviour prediction.

Acknowledgements
This work was funded by the Spanish CICYT (Grant MAT97-0442) and Xunta de Galicia (Grants XUGA 11801B95 and XUGA 11802B97). One of the authors (VKh) is indebted to Xunta de Galicia and DGICYT (Grants SAB95-0122 and SAB95-0122P) for supporting his stays, respectively, as a visiting scientist and sabbatic professor at the University of La Coruña.

REFERENCES

1. Suresh, S., *Fatigue of Materials*, Cambridge University Press, Cambridge (UK), 1991.
2. Kanninen, M.F. and Popelar, C.H., *Advanced Fracture Mechanics*, Oxford University Press, New York , 1985.
3. Rice, J.R., Mechanics of crack tip deformation and extension by fatigue, in: *Fatigue Crack Propagation, ASTM STP 415*, American Society for Testing and Materials, 1967, pp. 247-309.
4. McClung, R.C. and Sehitoglu, H., On the finite element analysis of fatigue crack closure. —1. Basic modeling issues. —2. Numerical results. *Engng Fracture Mech.* 1989, **33**, 237-272.
5. McClung, R.C., Crack closure and plastic zone sizes in fatigue. *Fatigue and Fract. Engng Mater. and Struct.* 1991, **14**, 455-468.
6. McClung, R.C., Thacker, B.H. and Roy, S., Finite element visualisation of fatigue crack closure in plane stress and plane strain. *Int. J. Fracture* 1991, **50**, 27-49.
7. Llorca, J. and Sánchez Gálvez, V., Modelling plasticity-induced fatigue crack closure. *Engng Fracture Mech.* 1990, **37**, 185-196.
8. Ellyin, F. and Wu, J., Elastic-plastic analysis of a stationary crack under cyclic loading and effect of overload. *Int. J. Fracture* 1992, **56**, 189-208.
9. Wu, J. and Ellyin, F., A study of fatigue crack closure by elastic-plastic finite element analysis for constant amplitude loading. *Int. J. Fracture* 1996, **82**, 43-65.
10. Gortemaker, P.C.M., de Pater, C. and Spiering, R.M.E.J., Near-crack tip finite strain analysis, in: *Advances in Fracture Research (Proceedings of the 5th International Conference on Fracture, Cannes, 1981)*, Vol. 1, Pergamon Press, Oxford, 1981, pp. 151-160.
11. McMeeking, R.M., Finite deformation analysis of crack tip opening in elastic-plastic materials and implications for fracture. *J. Mech. Phys. Solids* 1977, **25**, 357-381.
12. Handerhan, K.J. and Garrison, W.M., Jr., A study of crack tip blunting and the influence of blunting behavior on the fracture toughness of ultra high strength steels. *Acta Metall. Mater.* 1992, **40**, 1337-1355.
13. Savruk, M.P., *Stress Intensity Factors in Solids With Cracks*, Naukova Dumka, Kiev, 1988 (in Russian).
14. McMeeking, R.M. and Parks, D.M., On criteria of *J*-dominance of crack-tip fields in large-scale yielding, in: *Elastic-Plastic Fracture, ASTM STP 668*, American Society for Testing and Materials, 1979, pp. 175-194.
15. MARC User Information, Marc Analysis Research Corporation, Palo Alto, 1994.
16. Ritchie, R.O., Knott, J.F. and Rice, J.R., On the relationship between critical tensile stress and fracture toughness in mild steel. *J. Mech. Phys. Solids* 1973, **21**, 395-410.
17. Stout, M.G. and Gerberich, W.W., Structure/property/continuum synthesis of ductile fracture in Inconel alloy 718. *Met. Trans.* 1978, **A9**, 649-658.